CLIMATOLOGY

Collapse of the Liangzhu and other Neolithic cultures in the lower Yangtze region in response to climate change

Haiwei Zhang[1,2]*, Hai Cheng[1,2,3]*, Ashish Sinha[4], Christoph Spötl[5], Yanjun Cai[1,2], Bin Liu[6], Gayatri Kathayat[1], Hanying Li[1], Ye Tian[1], Youwei Li[1], Jingyao Zhao[1], Lijuan Sha[1], Jiayu Lu[1], Binglin Meng[1], Xiaowen Niu[1], Xiyu Dong[1], Zeyuan Liang[1], Baoyun Zong[1], Youfeng Ning[1], Jianghu Lan[2], R. Lawrence Edwards[7]

The Liangzhu culture in the Yangtze River Delta (YRD) was among the world's most advanced Neolithic cultures. Archeological evidence suggests that the Liangzhu ancient city was abandoned, and the culture collapsed at ~4300 years ago. Here, we present speleothem records from southeastern China in conjunction with other paleoclimatic and archeological data to show that the Liangzhu culture collapsed within a short and anomalously wet period between 4345 ± 32 and 4324 ± 30 years ago, supporting the hypothesis that the city was abandoned after large-scale flooding and inundation. We further show that the demise of Neolithic cultures in the YRD occurred within an extended period of aridity that started at ~4000 ± 45 years ago. We suggest that the major hydroclimatic changes between 4300 and 3000 years ago may have resulted from an increasing frequency of the El Niño–Southern Oscillation in the context of weakened Northern Hemisphere summer insolation.

INTRODUCTION

Rice-based agriculture in the lower Yangtze region has played a vital role in shaping the Chinese dynastic and predynastic civilizations throughout the past 5 millennia (1–3). Archeological studies over the past three decades have well established the Neolithic archeological sequence in the lower Yangtze region (1–3), which includes (i) the Shangshan [c. 10 to 8.5 thousand years before the present (ka B.P.)], the Kuahuqiao (c. 8.5 to 7.3 ka B.P.), and the Hemudu (c. 7.3 to 5.3 ka B.P.) cultures in the southern Hangzhou Bay; and (ii) the Majiabang-Songze (c. 7.3 to 5.3 ka B.P.), the Liangzhu (c. 5.3 to 4.3 ka B.P.), and the Qianshanyang-Guangfulin (c. 4.3 to 4.0 ka B.P.) cultures in the Yangtze River Delta (YRD) (see text S1.1 and fig. S1C). Of all Neolithic cultures, the Liangzhu culture was, perhaps, the most materially and technologically advanced (1–3), consisting of a large "capital city" with palaces and inner and outer city walls (~4× the size of the Forbidden City in Beijing) with an elaborate water management system (~5.1 ka B.P.) (4) and a sophisticated jade industry (text S1.2 and figs. S1E and S2) (1–3). As documented by many archeological sites across the YRD, the capital city, ruins of which were recently inscribed as a World Heritage Site (5), was abandoned, and the Liangzhu culture collapsed at ~4.3 ka B.P. (2, 3). The demise of this culture has been attributed to catastrophic climate and/or environmental events such as fluvial floods (1, 6–9), marine inundation caused by super typhoon events (10) or marine transgression (11) accompanying accelerated sea level rise, frequent cycles of droughts

and floods (12), extremely cold temperatures or cold-wet climate (13–15), military conflicts, and changes in the social structure (6, 9). Most archeological studies, however, support the flood hypothesis as evidenced by a layer of silt (interpreted as a flood deposit of either fluvial or marine origin) that caps the late Liangzhu cultural layer in many excavation sites (fig. S3) (2, 9).

In this study, we present new precisely dated and highly resolved speleothem records from Shennong and Jiulong caves near the YRD together with other paleoclimatic and archeological data that provide evidence in support of the hypothesis of flooding and inundation. Our data also provide new insights into how climate change may have affected the evolution of the other Neolithic cultures in the region.

RESULTS

Modern climatology

Shennong [117.25°E, 28.7°N, 383 m above sea level (a.s.l.)] and Jiulong (113.9°E, 27.8°N, 162 m a.s.l.) caves are located in the middle-lower reaches of the Yangtze River Valley (YRV) (Fig. 1 and fig. S1), ~350 km southwest (SW) of the central area of Neolithic sites in the YRD (i.e., the Liangzhu ancient city; Fig. 1 and fig. S1). The regional climate is dominated by the East Asian summer monsoon (EASM), and precipitation is strongly modulated by the El Niño–Southern Oscillation (ENSO) (Fig. 1). Instrumental data show that the rainfall in the study area is representative of the wider region of the middle-lower reaches of the YRV, including the site of Liangzhu ancient city (fig. S4A). At the EASM onset, rainfall in mid-May and June results in regular flooding in the lower reaches of the YRV. In mid-July and August, the northward movement of the EASM rain belt results in a hot and relatively dry climate in this region. The summer rainfall also shows strong interannual variability related to changes in the EASM strength and ENSO teleconnections over the western tropical Pacific (16–18). When the strength of the EASM decreases, the southward migration of the rain belt leads to

[1]Institute of Global Environmental Change, Xi'an Jiaotong University, Xi'an 710054, China. [2]State Key Laboratory of Loess and Quaternary Geology, Institute of Earth Environment, Chinese Academy of Sciences, Xi'an 710061, China. [3]Key Laboratory of Karst Dynamics, Ministry of Land and Resources, Institute of Karst Geology, Chinese Academy of Geological Sciences, 541004 Guilin, China. [4]Department of Earth Science, California State University Dominguez Hills, Carson, CA 90747, USA. [5]Institute of Geology, University of Innsbruck, Innsbruck 6020, Austria. [6]School of Art and Archaeology, Zhejiang University, Hangzhou 310028, China. [7]Department of Earth Sciences, University of Minnesota, Minneapolis, MN 55455, USA.
*Corresponding author. Email: cheng021@xjtu.edu.cn (H.C.); zhanghaiwei@xjtu.edu.cn (H.Z.)
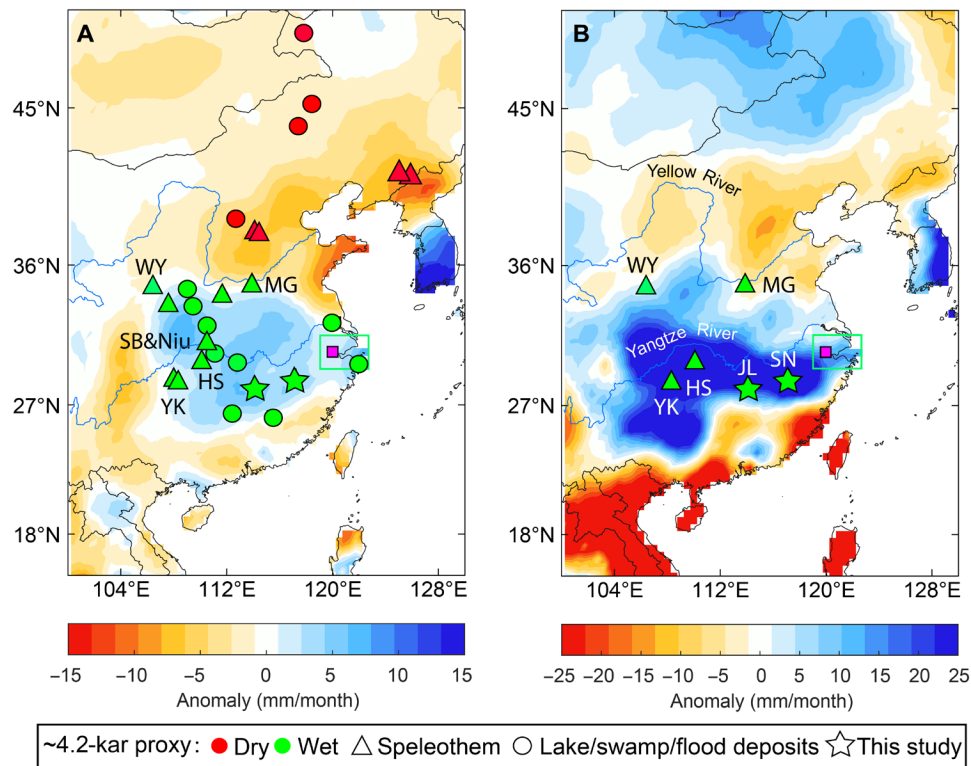
Fig. 1. Modern climatology and location of climate proxy sites as discussed in this study. (**A**) JJAS rainfall anomalies during the weakened EASM period between 1979 and 2010 CE relative to the interval 1951–2015 CE. (**B**) JJAS rainfall anomalies during the decaying phase of the 1982/1983, 1987/1988, 1992/1993, 1997/1998, and 2006/2007 El Niño events. The monthly spatial rainfall amount data (1951–2015) were obtained from the Climatic Research Unit (CRU TS v4; https://crudata.uea.ac.uk/cru/data/hrg/) with a grid resolution of 1° × 1°. Also shown are the locations of paleoclimate archives in eastern China recording a change in hydroclimate around the 4.2 ka B.P. event (between 4.2 and 3.9 ka B.P.; table S1). Green rectangle and pink square indicate the main Neolithic sites in the YRD and the Liangzhu capital city, respectively. JL: Jiulong cave; SN: Shennong cave; WY: Wuya cave; MG: Magou cave; SB & Niu-Sanbao and Niu caves; HS: Heshang cave; YK: Yangkou cave (table S1).

less summer monsoon rainfall [June-July-August-September (JJAS)] in northern China but more rainfall in the middle and lower reaches of the YRV (Fig. 1A). The waning phase of El Niño generally results in more JJAS rainfall and associated flooding in the middle and lower reaches of the YRV (Fig. 1B) (16, 19). In addition, increased typhoon intensity and super typhoon occurrence in summer are observed during El Niño years (20, 21). At present, the low-lying land on both sides of Hangzhou Bay is often subject to severe flooding caused by intense rainfall, typhoons, and poor drainage during the summer monsoon season (22).

Paleoclimatic records

We previously reported composites of multiple (stalagmite SN29, SN31, and SN35) speleothem oxygen (δ^{18}O) and carbon (δ^{13}C) isotope records from Shennong cave (Fig. 2, A and B) (23). In this study, we present additional δ^{18}O and δ^{13}C data from stalagmite SN17 with improved dating precision [~25-year average age error (2σ)] and temporal resolution (~3 years) (Fig. 2, A and B, and fig. S5) (24). In addition, we report new δ^{18}O and δ^{13}C records of stalagmite JL1 from Jiulong cave (Fig. 2, C and D), ~200 km SW of the Shennong cave (Fig. 1). The JL1 record is based on ~500 δ^{18}O and δ^{13}C measurements and 15 ^{230}Th dates, with an average temporal resolution of ~14 years (Fig. 2 and fig. S5). The δ^{18}O and δ^{13}C records show coherent variations between the two caves (text S1.3 and figs. S6 and S7), suggesting that these stalagmites were likely formed under

conditions close to isotope equilibrium according to the "replication test" (25). We interpret δ^{18}O and δ^{13}C changes to reflect hydroclimate variations rather than local kinetic effects (e.g., evaporation inside the cave, before calcite precipitation).

Previous studies have suggested that speleothem δ^{18}O in the EASM domain reflects the overall EASM intensity associated with changes in large-scale monsoon circulation and concomitant latitudinal shifts of the monsoon rain belt, with lower δ^{18}O implying higher spatially integrated monsoon rainfall between the tropical monsoon sources and the cave site and/or higher summer monsoon rainfall in the cave region (17, 23, 26, 27). However, speleothem δ^{18}O in southeastern China cannot always be used as a proxy of local rainfall amount because its main influencing factors (e.g., rainfall amount, precipitation seasonality, and moisture source) are time scale dependent (text S1.3 and fig. S8) (23). Therefore, to exclude nonprecipitation effects (e.g., changes in moisture source or precipitation seasonality) on speleothem δ^{18}O in the study area (23, 28), we have used speleothem δ^{13}C as a primary hydroclimate proxy in this study. Although some studies found that CO_2 degassing in the epikarst and inside the cave and/or strong cave ventilation can result in kinetic isotope fractionation and thus substantially influence speleothem δ^{13}C values (29, 30), it has been suggested that under conditions close to isotope equilibrium, the speleothem δ^{13}C is primarily controlled by the vegetation (e.g., C3/C4 type and vegetation density) responding to regional hydroclimate variations (24, 30, 31).
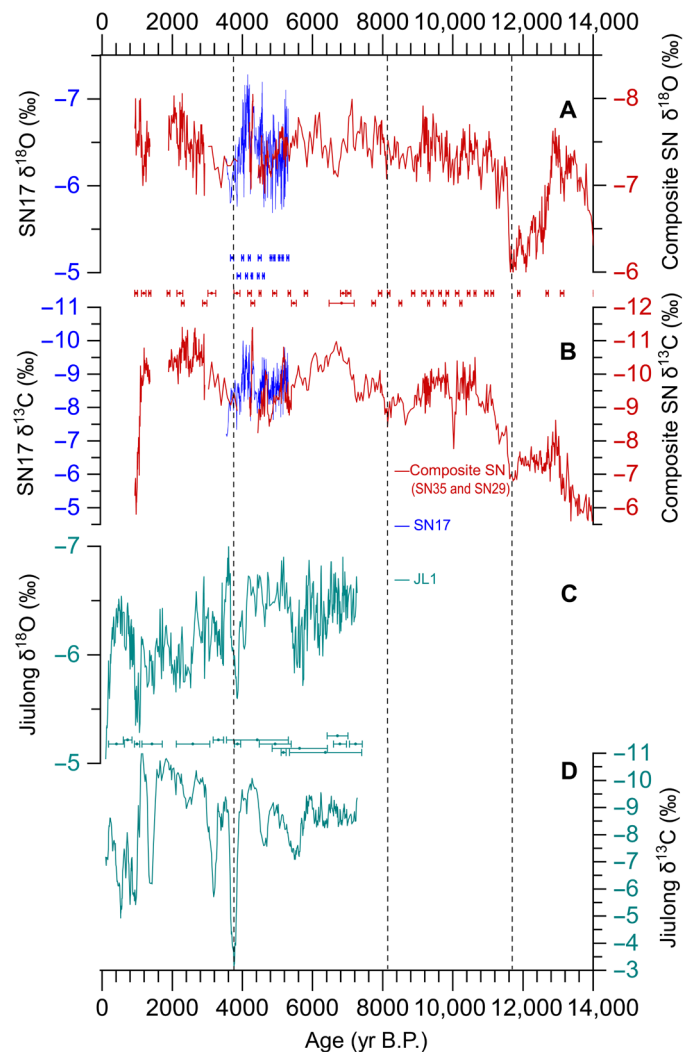
Fig. 2. Comparison of speleothem records from Shennong and Jiulong caves. (**A**) Composite Shennong δ^{18}O (red) (*23*) and SN17 δ^{18}O (blue) records from Shennong cave. ‰: per mil. (**B**) Composite Shennong δ^{13}C (red) and SN17 δ^{13}C (blue) records from Shennong cave. (**C**) JL1 δ^{18}O record from Jiulong cave. (**D**) JL1 δ^{13}C record from Jiulong cave. [230]Th dates are shown with their 2σ errors. The dashed black lines indicate three periods with higher values of δ^{18}O and δ^{13}C in both Shennong and Jiulong caves. Note inverted *y* axes.

On the basis of pollen and organic δ^{13}C of lacustrine sediments, it has been demonstrated that there has been no significant change in vegetation type (dominated by C3 vegetation) in the lower reaches of the YRV during the Early-Middle Holocene (*32–34*). Speleothem δ^{13}C in the study area is, thus, mainly influenced by the vegetation density associated with hydroclimate change during the Holocene, with higher (lower) speleothem δ^{13}C values corresponding to relatively dry (wet) climate (*24, 30, 31*).

The δ^{13}C records of Shennong and Jiulong caves show coherent variations (fig. S6), indicating that these records reflect the regional hydroclimate. The different δ^{13}C values of stalagmites in Shennong and Jiulong caves might be caused by differences in the proportion of seepage versus fracture flow feeding the stalagmites (*23, 35*). Excluding kinetic fractionation effects on speleothem samples from

Shennong and Jiulong caves, covarying δ^{13}C and δ^{18}O values in both Shennong (*r* = 0.64, *P* < 0.01, *n* = 725) and Jiulong (*r* = 0.20, *P* < 0.01, *n* = 505) records on decadal-to-centennial time scales indicate that speleothem δ^{18}O in the study area may also reflect hydroclimate changes on these time scales (text S1.3 and fig. S7) (*30*).

A long-term decreasing trend of Shennong and Jiulong δ^{13}C during the Holocene indicates a gradual increase in precipitation in the lower reaches of the YRV (Fig. 3, E and F). The trend is punctuated by two millennial-scale positive excursions (9 to 8 ka B.P. and 4.5 to 3 ka B.P.; light yellow bars in Fig. 3, E and F), consistent with the timing of two hiatuses in a stalagmite from Niu cave from the middle reaches of the YRV (Figs. 1 and 3D) and with drier periods inferred from other proxy reconstructions of rainfall (*12, 34*) from the middle-lower reaches of the YRV (fig. S9). Of note is an abrupt excursion toward a wet climate between 4.3 and 4.0 ka B.P. followed by an abrupt dry event between 4.0 and 3.6 ka B.P., a wet period between 3.6 and 3.3 ka B.P., and another dry period between 3.3 and 3.0 ka B.P. (Fig. 3, E and F), which can be also observed in the Yangkou cave δ^{13}C record (Fig. 3D) from the middle reaches of the YRV, indicating unstable climatic conditions between 4.3 and 3.0 ka B.P. in the region. Periods of "megadrought" and "pluvial event" conditions are defined by δ^{13}C *z* score values higher and lower than 1σ for at least 15 consecutive years, respectively (Fig. 4, D and E). Our definition of a megadrought is similar to the previous usage of this term (*30*). In the past 1.5 ka, the δ^{13}C values of the speleothems from Shennong and Jiulong caves were largely influenced by increased anthropogenic disturbance (*29*), not relevant for this study (Fig. 3, E and F).

DISCUSSION
Climatic context of the pre-Liangzhu Neolithic cultures
To better understand the rise and fall of the Liangzhu culture, we first introduce briefly the climate background and its possible influences on the evolution of the Neolithic cultures before the Liangzhu culture (Fig. 3G). The Shennong cave δ^{13}C record, together with other nearby paleorainfall records (*12, 34*), suggests that wet and stable climatic conditions prevailed for ~1500 years during the Shangshan culture (c. 10 to 8.5 ka B.P.) (Fig. 3, E and G). The transition from the Shangshan to the Kuahuqiao culture (c. 8.5 to 7.3 ka B.P.) may have occurred in response to a multicentennial dry period centered at ~8.5 ka B.P. (Fig. 3, E and G) because most Kuahuqiao sites are found at lower elevations near the river compared to Shangshan sites (fig. S1C) (*3*). The initial occupation of the Kuahuqiao sites at South Hangzhou Bay was also likely related to the initial formation of the coastal plain at the apex of South Hangzhou Bay (*36, 37*). The short duration of the Kuahuqiao culture might be partly related to a transition from a drier to a wetter climate. Alternatively, some previous studies have also suggested that sea level rise and extreme events such as storms and flooding might have restricted the duration of the Kuahuqiao culture (*3, 36*). The subsequent Hemudu and Majiabing-Songze cultures (c. 7.3 to 5.3 ka B.P.) thrived during the Holocene rainfall optimum (Fig. 3, D to G), as archeological data show that the rice cultivation reached a relatively high level by ~6.6 ka B.P. [e.g., (*37, 38*)]. These cultures may have further benefited from the progradation of the coastal plain because of a gradually stabilizing sea level and huge sediment input from the Yangtze and Qiantang rivers under a wet climate (*3, 22, 39*), consistent with a large number of Neolithic relics in the YRD (Fig. 3H) (*7*).
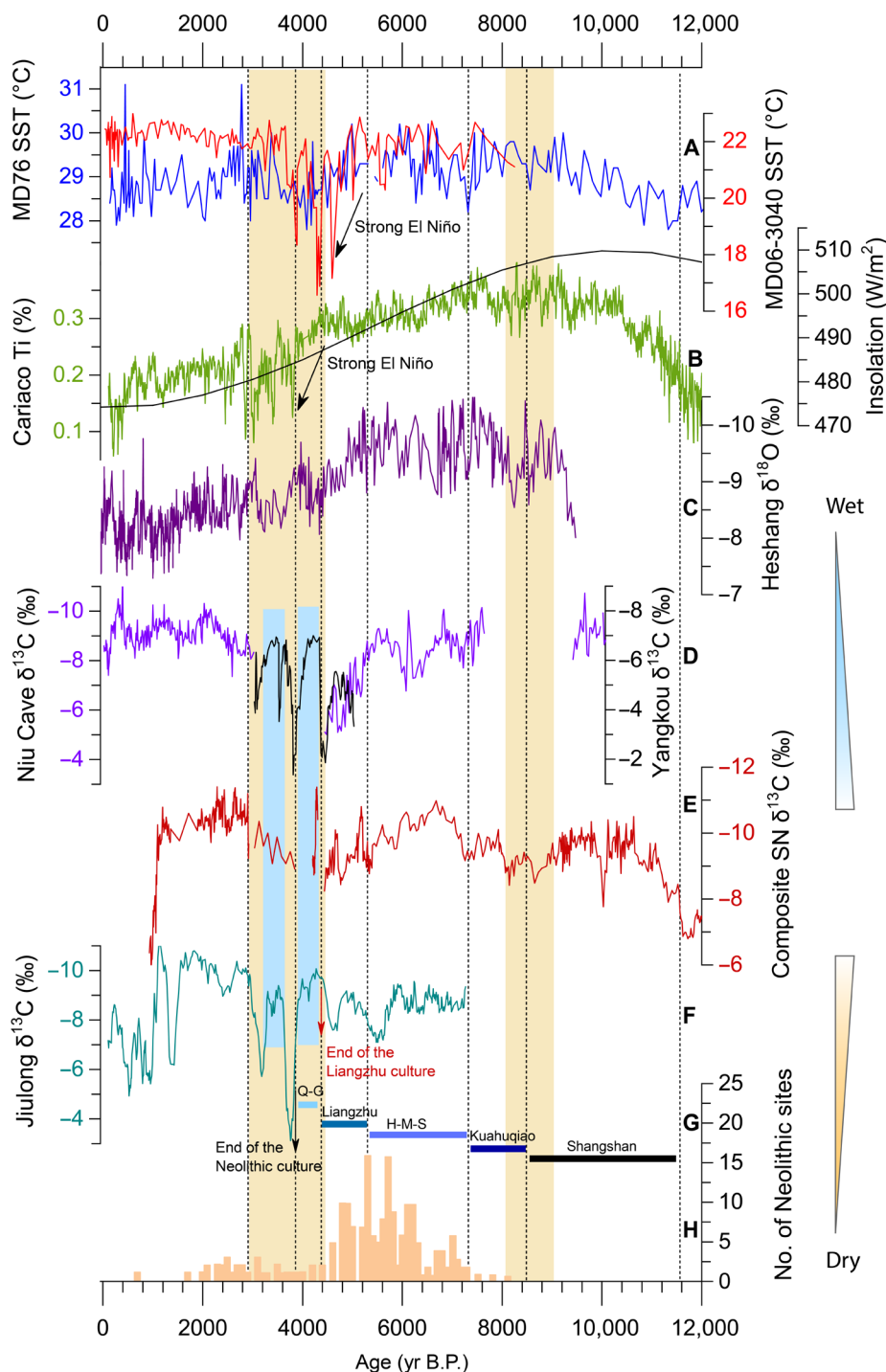
Fig. 3. Speleothem records in comparison with other paleoclimate data and the cultural history in the lower Yangtze region. (**A**) Sea surface temperature (SST) records from western Pacific core MD06-3040 (*13*) and MD76 (*56*). (**B**) Cariaco basin sediment Ti concentration (*57*) and July insolation at 65°N (black curve) (*58*). (**C**) Heshang cave $\delta^{18}O$ (*59*). (**D**) Niu cave (*31*) and Yangkou cave (*60*) $\delta^{13}C$ records. (**E**) Composite SN $\delta^{13}C$ record from Shennong cave (this study). (**F**) JL1 $\delta^{13}C$ record from Jiulong cave (this study). (**G**) Succession of Neolithic cultures (Q-G: Qianshanyang-Guangfulin cultures; H-M-S: Hemudu and Majiabang-Songze cultures) (*1*, *3*). (**H**) Neolithic excavation sites in the YRD (*7*). Light yellow and blue bars indicate droughts and pluvial periods, respectively.

We acknowledge that the interaction between sea level rise and the progradation of the YRD might also have played an important role in the cultural evolution during the Early Holocene (text S1.1) (*3*, *22*, *39–41*). By 6.0 ka B.P., the sea level had largely stabilized, and the YRD was essentially established (fig. S3D) (*3*, *22*, *39*); thus, changes in regional hydroclimate became a more critical influencing factor on the evolution of the Liangzhu and subsequent Qianshanyang-Guangfulin cultures.
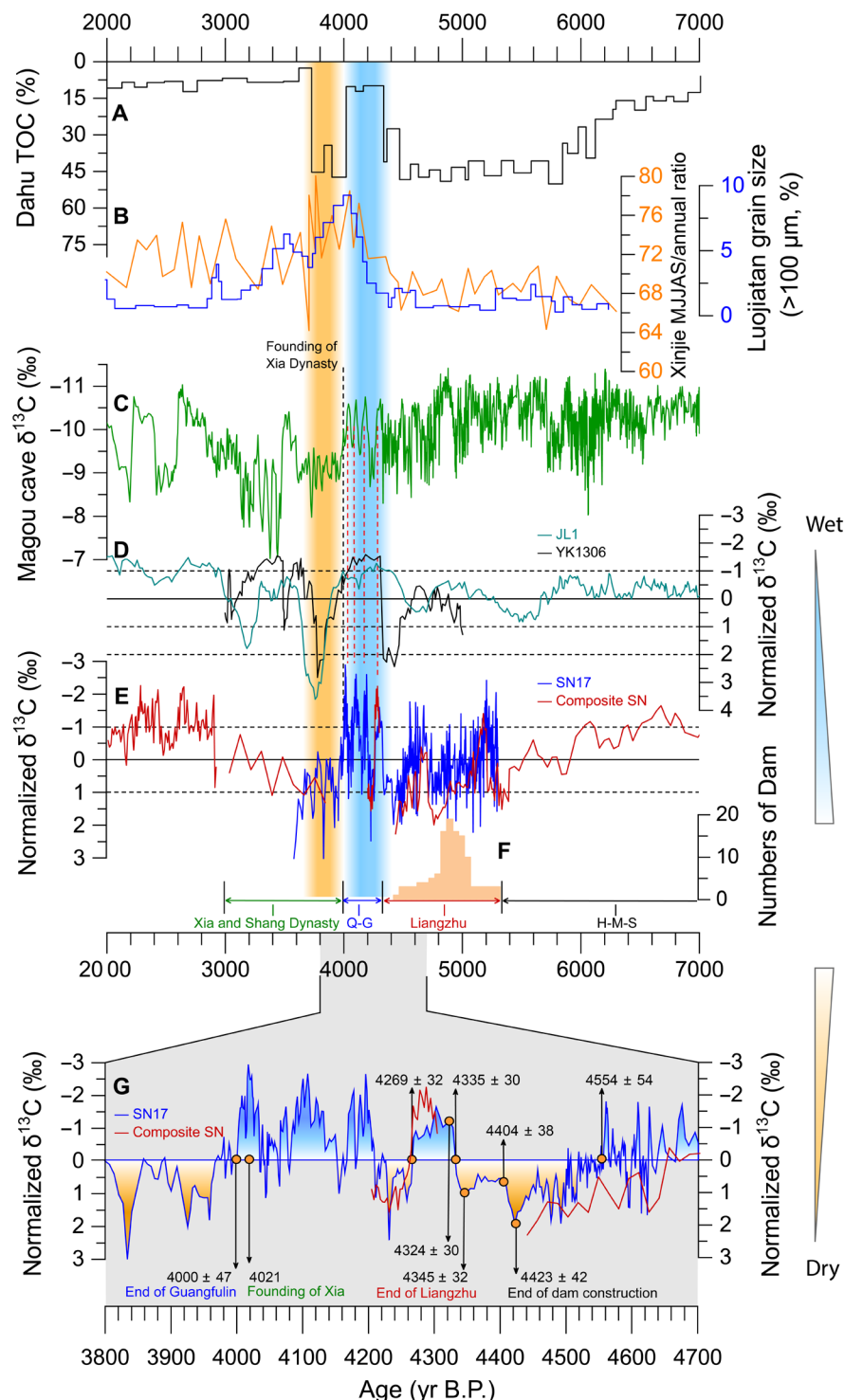
Fig. 4. Speleothem records in comparison to rainfall/humidity records from flood deposits, peat sediments, and archeological data. (**A**) Total organic carbon (TOC) concentration from Dahu peat sediment in southeastern China (*32*). (**B**) Overbank flooding events inferred from the >100-μm sand fraction in a Holocene loess-soil profile (blue) (*61*) and pollen-reconstructed MJJAS (May-June-July-August-September)/annual rainfall ratio from peat sediments (orange) (*12*) in the middle and lower reaches of the YRV. (**C**) Speleothem $\delta^{13}C$ record from Magou cave, central China (*35*). (**D**) Normalized Jiulong (this study) and Yangkou (*60*) cave $\delta^{13}C$ records. (**E**) Normalized speleothem $\delta^{13}C$ records from Shennong (composite SN and SN17, this study) cave. (**F**) Archeological data of the hydraulic construction (numbers of dams) by the Liangzhu people (*4*). (**G**) The inset shows the Shennong cave $\delta^{13}C$ records between 3.8 and 4.7 ka B.P. and the major historical events delineated by black vertical arrows in (G). Red dashed lines mark the four wet episodes inferred from the Shennong (E) and Magou (D) cave records. Blue and yellow zones indicate wet and dry periods, respectively. Black vertical dashed line in (C) to (E) indicates the founding of the Xia Dynasty at 4021 yr B.P.

Collapse of the Liangzhu culture

Liangzhu city was built at the head of an embayment backed by hills, with close access to fresh water and timber. This location afforded the city protection from coastal hazards after the wetlands had changed from salt water to fresh water in response to rapid coastal progradation as the postglacial sea level rise stabilized (40). The Shennong $\delta^{13}C$ record suggests that the emergence of the Liangzhu culture coincided with the onset of a dry interval around 5.3 ka B.P. (Fig. 4E). As mentioned above, the Liangzhu site is located in a low-lying region with strong variability in precipitation, where flooding normally occurs in June followed by a dry and hot July–August. Archeological studies show the presence of large-scale hydraulic complexes such as large earthen dams near the Liangzhu city (4), which were constructed between 5.3 and 4.7 ka B.P. (Fig. 4F and text S1.2) (4). This suggests that the Liangzhu society was effectively managing water resources by using hydraulic infrastructure for flood mitigation and/or irrigation to survive in a dry climate (4, 40). The dam construction terminated around 4.4 ka B.P. (Fig. 4, E and F), which may be related to a megadrought at 4423 ± 42 yr B.P. (Fig. 4, E to G). It was the driest period in the Liangzhu cultural history, consistent with hiatuses in composite SN and Niu cave records (Fig. 3, D and E) and paleorainfall changes observed in other proxy records nearby (fig. S9) (12, 34). The proxy-inferred multi-centennial drier conditions during the late Liangzhu cultural period support archeological findings such as a lower absolute altitude of wells for drinking water in the Liangzhu relics (42, 43) and significant contractions in lake areas and depths (text S1.2) (6). An increase in charcoal frequency and pollen evidence of substantial deforestation in the YRD indicate that human activities were still high during the late Liangzhu period (6). Therefore, the termination of dam construction appears to relate to the megadrought around 4.4 ka B.P. (Fig. 4, E and F), because the existing dams were fully sufficient under such dry climate conditions.

Our data show that the drier conditions were punctuated by two pulses of pluvial conditions from 4423 ± 42 to 4404 ± 38 yr B.P. and between 4345 ± 32 and 4324 ± 30 yr B.P., with the latter marking the termination of the ~220-year drier condition between 4554 ± 54 and 4335 ± 30 yr B.P. (Fig. 4, E to G). The first pluvial episode is consistent with the age of the first flood sediment layer (4510 ± 100 yr B.P.) covering the Liangzhu culture layer north of the Liangzhu city and in the nearby Yushan site based on ^{14}C and single-grain optically stimulated luminescence ages (fig. S3, A and B) (10, 40). The second pluvial pulse coincided with the demise of the Liangzhu culture in the YRD centered at ~4300 yr B.P. based on a large archeological dataset (3, 10). This timing also coincides with the age of the second flood layer (4365 ± 80 yr B.P.) covering the Liangzhu culture layer at the Yushan site (fig. S3, B and C) (10). The second pluvial episode and the subsequent period from 4335 ± 30 to 4269 ± 32 yr B.P. were anomalously wet and unprecedented in the Liangzhu cultural history (Fig. 4, A, B, E, and G), which may have destroyed the hydraulic complex and wrecked the rice cultivation because of inundation of the low-lying land (Fig. 4, E to G). Our speleothem records, together with geochemical evidence of flood deposits above the Liangzhu culture layer (11), suggest that massive rainfall in the entire middle-lower reaches of the YRV might have induced fluvial flooding and/or overbank marine flooding transported by the Yangtze River plume and thus impeded human habitation and rice farming on both sides of the Hangzhou Bay, especially the Taihu Plain region of the YRD (2, 3, 7, 14). Some sites (e.g., Yushan) close to the coastline may also

have been subjected to marine flooding caused by typhoons and tidal storms (10). Therefore, we suggest that massive flooding and inundation due to poor drainage in the low-lying land may have forced the Liangzhu people to abandon their capital city and dwellings in the Taihu Plain, ultimately leading to the collapse of the entire Liangzhu civilization. In short, our new data provide a precise climatic framework that allows us to assess the climate impact on the collapse of the Liangzhu culture.

Demise of the Neolithic cultures in the YRD

After the Liangzhu culture had collapsed, the Qianshanyang-Guangfulin cultures briefly existed between 4.3 and 4.0 ka B.P. (Fig. 3G). Compared to their predecessor, these cultures were technologically less advanced (2, 3, 14). During this period, the Shennong speleothem $\delta^{13}C$ record clearly shows strong multidecadal climate variability marked by four wet and three dry intervals (Fig. 4E), consistent with a high-resolution speleothem $\delta^{13}C$ record from Magou cave in central China (Fig. 4C). It was also reported that an expansion of wetland with elevated water level (6, 36, 40) and a freshwater environment had covered an area two to three times the present Taihu basin during the late period of the Liangzhu culture and the later cultures (14, 15), consistent with the speleothem $\delta^{13}C$-inferred anomalously wet climate between 4.3 and 4.0 ka B.P. (Fig. 4, D to G). This wet climate might have had a significant impact on the rice agriculture during this episode (2, 3). Both Shennong and Jiulong $\delta^{13}C$ records indicate a megadrought at 4.0 ka B.P. (Fig. 4, D, E, and G), with the latter indicating the driest period of the entire Holocene around 3.8 ka B.P. (Figs. 3F and 4, D to G), synchronous with the collapse of the Qianshanyang-Guangfulin cultures (3). Other geological and archeological data in southern China also show evidence of this dry event (44), thus supporting our hypothesis that the collapse of Qianshanyang-Guangfulin cultures was caused by a megadrought. Following the Qianshanyang-Guangfulin cultures, only a few Neolithic sites are known to have existed in the YRD until the beginning of Shang and Zhou dynasties at ~3.0 ka B.P. (Fig. 3G). This ~1000-year-long cultural gap (3, 6) may be related to unstable climatic conditions including two megadroughts and one pluvial period documented in our speleothem and other paleorainfall records (Figs. 3 and 4), which presumably have hampered the cultural recovery in the region (15). It is thus apparent that the megadrought around 4.0 ka B.P. and the ensuing unstable climate until 3.0 ka B.P. might have brought this chapter of the Neolithic culture to the end in the YRD.

The onset of the megadrought coincides with the founding of the Xia Dynasty at 2070 BCE (4021 yr B.P.), which is considered as the first dynasty of China (45). While many documents indicate that the leader Yu built the Xia Dynasty because he successfully managed river flooding, some studies suggest that Yu's control of the flooding can be ascribed to climate change on the basis of the archeological data and climate reconstructions (8, 46). The high-resolution speleothem $\delta^{13}C$ records from Shennong, Jiulong, and Magou caves (Fig. 4, C to G; as well as speleothem $\delta^{18}O$ records from these caves, fig. S8) all show a wet-dry transition at 4000 ± 47 yr B.P. in a large part of central China between the southern middle-lower Yellow River and the middle-lower Yangtze River (Fig. 1), the main activity region of the Xia Dynasty (45). This observation provides new robust evidence that the rise of the Xia Dynasty occurred in the context of a major climate transition from wet to dry, in line with the Chinese historic records and previous studies (8, 9, 46, 47).

Possible mechanism(s) of climate change between 4.3 and 3.0 ka B.P.

Holocene climate change in eastern China has been shown to be primarily controlled by variations in the EASM strength driven by North Hemisphere summer insolation (NHSI) and also strongly modulated by the increased ENSO variance since the Middle and Late Holocene [e.g., (23, 31, 35, 44, 48, 49)]. In the context of NHSI and EASM waning during the mid-Holocene, the southward shift of the EASM rain belt and intertropical convergence zone (ITCZ) may have led to relatively increased rainfall in the middle-lower reaches of the YRV and decreased rainfall in northern China (Fig. 3), similar to the "northern dry and southern wet" pattern observed during the instrumental weak EASM periods (Fig. 1A) (23). It has been suggested that the northern dry and southern wet pattern around 4.2 ka B.P. might have been caused by the cold climate in the North Atlantic characterized by increased ice-rafted debris (fig. S9) (24, 49) associated with the weakened EASM intensity and the southward migration of the ITCZ caused by cooler sea surface temperatures (SSTs) of the North Atlantic. However, the strong variability on decadal-centennial time scales between 4.3 and 3.0 ka B.P. cannot be fully explained by either insolation forcing or northern high-latitude forcing.

Previous studies suggest that an intensified ENSO over the Holocene (50) may have resulted in high-frequency climate change in eastern China (31, 44, 48). Instrumental data also show that during the decaying phase of El Niño, colder SSTs of the West Pacific lead to anomalous cyclonic circulation and moisture convergence over the YRV at the lower troposphere, resulting in more rainfall and flood events in the YRV (Fig. 1B) (16). The comparison with Holocene tropical SSTs of the West Pacific (Fig. 3A) suggests that significantly increased El Niño events in the context of the southward migration of the monsoonal rain belt caused by the weakened EASM may have caused the frequent flooding between 4.3 and 4.0 ka B.P. (Figs. 3 and 4). Abrupt decreases in $\delta^{18}O$ in Shennong, Jiulong, and Yangkou records (Fig. 2, A and C, and fig. S8) indicate that this high rainfall was mainly concentrated in summer because monsoon rainfall results in lower $\delta^{18}O$ values of precipitation (text S1.3). This is further supported by the high MJJAS (May-June-July-August-September)/annual precipitation ratio inferred from pollen data and the overbank flooding events in summer inferred from a Holocene loess-soil profile in the middle-lower reaches of the YRV (Fig. 4B). This implies that frequent ENSO co-occurring with the weakened EASM led to repeated and/or concentrated summer floods in the middle-lower reaches of the YRV between 4.3 and 4.0 ka B.P., similar to the four largest destructive floods of the past 60 years that occurred in this region during the waning phase of El Niño (i.e., the summers in 1954, 1998, 2016, and 2000 CE) (Fig. 1B).

The chronologically well-constrained Shennong and Jiulong speleothems are currently the highest-resolution proxy records of the EASM from the middle-lower reaches of the YRV. Together with other proxy reconstructions of rainfall from the region, our data provide a continuous hydroclimate history over the past 14 ka against which the evolution of the Neolithic cultures in the lower Yangtze River can be more precisely assessed. In the context of coastal land formation on both sides of the Hangzhou Bay due to sea level rise and sediment transport from river catchment, the Hemudu and Majiabang-Songze cultures flourished during a humid climate and likely developed into the Liangzhu culture as a result of a drying course. Whereas the collapse of the highly developed Liangzhu culture might have been caused by flooding and inundation between 4345 ± 32 yr B.P. and 4324 ± 30 yr B.P., a megadrought starting at 4000 ± 47 yr B.P. and a subsequent volatile climate may have resulted in the final demise of the Neolithic culture in the YRD. The unstable climate between 4.3 and 3.0 ka B.P. was possibly caused by an increasing frequency of ENSO in the context of a gradual NHSI weakening. In addition, the speleothem $\delta^{13}C$-inferred wet-dry transition in central China between the southern middle-lower Yellow River and the middle-lower Yangtze River at 4000 ± 47 yr B.P. is consistent with the climate evolution and the timing of the founding of the Xia Dynasty. Our study provides important new climate change evidence for settling the dispute surrounding the collapse of the Liangzhu culture, the final demise of Neolithic cultures in the YRD, and the climate background of the founding of the first dynasty (Xia) in China. Although various factors would certainly have affected these chapters of the cultural history in the region, our precise correlations between the climate-culture changes suggest that climate had played an important role.

MATERIALS AND METHODS

Study caves and samples

Shennong and Jiulong caves are located in the central-western and northeastern Jiangxi province, southeastern China (Fig. 1). Shennong cave developed in Carboniferous limestone of the Chuan-shan and Huang-long groups, which are mostly composed of limestone interbedded with dolostone. Previous studies have documented that the occurrence of aragonite and calcite speleothems in the Shennong cave is essentially related to the Mg content of drip water dissolved from carbonate bedrock (dolomite/limestone) (24, 29). Jiulong cave has a total length of ~6 km, and speleothems collected from the cave are composed of calcite. Stalagmite samples SN29, SN17, and SN31 were collected at 200, 400, and 1800 m from the Shennong cave entrance, and JL1 was collected at 800 m from the Jiulong cave entrance, respectively. SN29, SN17, and SN31 are composed of aragonite, whereas SN35 and JL1 are composed of calcite, confirmed by x-ray diffraction analyses.

Dating method and age models

[230]Th samples were hand-drilled along the growth axis of halved stalagmite JL1 and spiked with a mixed [235]U-[233]U-[229]Th spike similar to that described by Edwards et al. (51). Separate uranium and thorium liquid extracts were measured using a multicollector inductively coupled plasma mass spectrometer at the Isotope Laboratory, Institute of Global Environmental Change, Xi'an Jiaotong University. Details about the instrumental setup are provided by Cheng et al. (52, 53). We adopted COPRA (Constructing Proxy Records from kthe dating uncertainties (2.5 and 97.5% quantile confidence limits) (fig. S5) (54). The temporal resolution of SN17 on COPRA age models ranges from 1 to 12 years, with an average resolution of ~2.75 years. The average temporal resolution of JL1 is ~14 years.

Stable isotope analyses

A total of ~725 oxygen and carbon isotope subsamples were micromilled at 0.2-mm intervals along the growth axis of JL1. A total of ~500 oxygen and carbon isotope subsamples were micromilled at 0.2- and 1-mm intervals along the growth axis of SN17. These subsamples were measured on a Thermo Fisher Delta V Plus isotope ratio mass spectrometer equipped with a GasBench II at the Institute

of Geology, University of Innsbruck (*55*). Results are reported relative to the Vienna Peedee Belemnite standard with an analytical precision of 0.08 and 0.06 per mil for $\delta^{18}O$ and $\delta^{13}C$, respectively (1σ).

SUPPLEMENTARY MATERIALS

Supplementary material for this article is available at https://science.org/doi/10.1126/sciadv.abi9275

REFERENCES AND NOTES

1. L. Liu, X. Chen, *The Archaeology of China: From the Late Paleolithic to the Early Bronze Age* (Cambridge Univ. Press, 2012).
2. Zhejiang Provincial Institute of Culture Relics and Archaeology, *A comprehensive Study of Liangzhu Ancient City* (Cultural Relics Press, Beijing, 2019).
3. H. Zheng, Y. Zhou, Q. Yang, Z. Hu, G. Ling, J. Zhang, C. Gu, Y. Wang, Y. Cao, X. Huang, Y. Cheng, X. Zhang, W. Wu, Spatial and temporal distribution of Neolithic sites in coastal China: Sea level changes, geomorphic evolution and human adaption. *Sci. China Earth Sci.* **61**, 123–133 (2018).
4. B. Liu, N. Wang, M. Chen, X. Wu, D. Mo, J. Liu, S. Xu, Y. Zhuang, Earliest hydraulic enterprise in China, 5,100 years ago. *Proc. Natl. Acad. Sci. U.S.A.* **114**, 13637–13642 (2017).
5. World Heritage List: Archaeological Ruins of Liangzhu City, United Nations Educational, Scientific and Cultural Organization (UNESCO); https://whc.unesco.org/en/list/1592.
6. Y. Zong, J. B. Innes, Z. Wang, Z. Chen, Mid-Holocene coastal hydrology and salinity changes in the east Taihu area of the lower Yangtze wetlands, China. *Quatern. Res.* **76**, 69–82 (2011).
7. Q. Zhang, C. Zhu, C.-L. Liu, T. Jiang, Environmental change and its impacts on human settlement in the Yangtze Delta, P.R. China. *Catena* **60**, 267–277 (2005).
8. W. Wu, Q. Ge, The possibility of occurring of the extraordinary floods on the eve of establishment of the Xia Dynasty and the historical truth of Dayu's successful regulating of floodwaters. *Quat. Sci.* **25**, 741–748 (2005).
9. W. Wu, T. Liu, 4000 a BP event and its implications for the origian of ancient Chinese civilization. *Quat. Sci.* **5**, 443–451 (2001).
10. Z. Wang, D. B. Ryves, S. Lei, X. Nian, Y. Lv, L. Tang, L. Wang, J. Wang, J. Chen, Middle Holocene marine flooding and human response in the south Yangtze coastal plain, East China. *Quat. Sci. Rev.* **187**, 80–93 (2018).
11. K. He, H. Lu, G. Sun, X. Ji, Y. Wang, K. Yan, X. Zuo, J. Zhang, B. Liu, N. Wang, Multi-proxy evidence of environmental change related to collapse of the Liangzhu Culture in the Yangtze Delta, China. *Sci. China Earth Sci.* **64**, 890–905 (2021).
12. F. Lu, C. Ma, C. Zhu, H. Lu, X. Zhang, K. Huang, T. Guo, K. Li, L. Li, B. Li, W. Zhang, Variability of East Asian summer monsoon precipitation during the Holocene and possible forcing mechanisms. *Climate Dynam.* **52**, 969–989 (2019).
13. H. Kajita, H. Kawahata, K. Wang, H. Zheng, S. Yang, N. Ohkouchi, M. Utsunomiya, B. Zhou, B. Zheng, Extraordinary cold episodes during the mid-Holocene in the Yangtze delta: Interruption of the earliest rice cultivating civilization. *Quat. Sci. Rev.* **201**, 418–428 (2018).
14. Z. Chen, Z. Wang, J. Schneiderman, J. Taol, Y. Cail, Holocene climate fluctuations in the Yangtze delta of eastern China and the Neolithic response. *Holocene* **15**, 915–924 (2005).
15. J. B. Innes, Y. Zong, Z. Wang, Z. Chen, Climatic and palaeoecological changes during the mid-to Late Holocene transition in eastern China: High-resolution pollen and non-pollen palynomorph analysis at Pingwang, Yangtze coastal lowlands. *Quat. Sci. Rev.* **99**, 164–175 (2014).
16. D. Jin, S. N. Hameed, L. Huo, Recent changes in ENSO teleconnection over the western Pacific impacts the eastern China precipitation dipole. *J. Climate* **29**, 7587–7598 (2016).
17. H. Zhang, H. Cheng, C. Spötl, Y. Cai, A. Sinha, L. Tan, L. Yi, H. Yan, G. Kathayat, Y. Ning, X. Li, F. Zhang, J. Zhao, R. L. Edwards, A 200-year annually laminated stalagmite record of precipitation seasonality in southeastern China and its linkages to ENSO and PDO. *Sci. Rep.* **8**, 12344 (2018).
18. C. Xu, J. Ge, T. Nakatsuka, L. Yi, H. Zheng, M. Sano, Potential utility of tree ring $\delta^{18}O$ series for reconstructing precipitation records from the lower reaches of the Yangtze River, southeast China. *J. Geophys. Res. Atmos.* **121**, 3954–3968 (2016).
19. W. Zhang, F.-F. Jin, M. F. Stuecker, A. T. Wittenberg, A. Timmermann, H.-L. Ren, J.-S. Kug, W. Cai, M. Cane, Unraveling El Niño's impact on the East Asian Monsoon and Yangtze River summer flooding. *Geophys. Res. Lett.* **43**, 11373–11382 (2016).
20. X. Feng, M. Li, Y. Li, F. Yu, D. Yang, G. Gao, L. Xu, B. Yin, Typhoon storm surge in the southeast Chinese mainland modulated by ENSO. *Sci. Rep.* **11**, 10137 (2021).
21. N.-Y. Kang, D. Kim, J. B. Elsner, The contribution of super typhoons to tropical cyclone activity in response to ENSO. *Sci. Rep.* **9**, 5046 (2019).
22. B. Dai, Y. Liu, Q. Sun, F. Ma, J. Chen, Z. Chen, Foraminiferal evidence for Holocene environmental transitions in the Yaojiang Valley, south Hangzhou Bay, eastern China, and its significance for Neolithic occupations. *Mar. Geol.* **404**, 15–23 (2018).

23. H. Zhang, X. Zhang, Y. Cai, A. Sinha, C. Spötl, J. Baker, G. Kathayat, Z. Liu, Y. Tian, J. Lu, Z. Wang, J. Zhao, X. Jia, W. Du, Y. Ning, Z. An, R. L. Edwards, H. Cheng, A data-model comparison pinpoints Holocene spatiotemporal pattern of East Asian summer monsoon. *Quat. Sci. Rev.* **261**, 106911 (2021).
24. H. Zhang, H. Cheng, Y. Cai, G. Kathayat, A. Sinha, R. L. Edwards, Hydroclimatic variations in southeastern China during the 4.2 ka event reflected by stalagmite records. *Clim. Past* **14**, 1805 (2018).
25. J. A. Dorale, Z. Liu, Limitations of Hendy test criteria in judging the paleoclimatic suitability of speleothems and the need for replication. *J. Caves Karst Stud.* **71**, 73–80 (2009).
26. H. Cheng, R. L. Edwards, A. Sinha, C. Spötl, L. Yi, S. Chen, M. Kelly, G. Kathayat, X. Wang, X. Li, X. Kong, Y. Wang, Y. Ning, H. Zhang, The Asian monsoon over the past 640,000 years and ice age terminations. *Nature* **534**, 640–646 (2016).
27. H. Cheng, H. Zhang, J. Zhao, H. Li, Y. Ning, G. Kathayat, Chinese stalagmite paleoclimate researches: A review and perspective. *Sci. China Earth Sci.* **62**, 1489–1513 (2019).
28. H. Zhang, H. Cheng, Y. Cai, C. Spötl, A. Sinha, G. Kathayat, H. Li, Effect of precipitation seasonality on annual oxygen isotopic composition in the area of spring persistent rain in southeastern China and its paleoclimatic implication. *Clim. Past* **16**, 211–225 (2020).
29. H. Zhang, Y. Cai, L. Tan, H. Cheng, S. Qin, Z. An, R. L. Edwards, L. Ma, Large variations of $\delta^{13}C$ values in stalagmites from southeastern China during historical times: implications for anthropogenic deforestation. *Boreas* **44**, 511–525 (2015).
30. H. Li, A. Sinha, A. A. André, C. Spötl, H. B. Vonhof, A. Meunier, G. Kathayat, P. Duan, N. R. G. Voarintsoa, Y. Ning, J. Biswas, P. Hu, X. Li, L. Sha, J. Zhao, R. L. Edwards, H. Cheng, A multimillennial climatic context for the megafaunal extinctions in Madagascar and Mascarene Islands. *Sci. Adv.* **6**, eabb2459 (2020).
31. K. Zhao, Y. Wang, R. L. Edwards, H. Cheng, D. Liu, X. Kong, Y. Ning, Contribution of ENSO variability to the East Asian summer monsoon in the late Holocene. *Palaeogeogr. Palaeoclimatol. Palaeoecol.* **449**, 510–519 (2016).
32. W. Zhou, X. Yu, A. J. T. Jull, G. Burr, J. Y. Xiao, X. Lu, F. Xian, High-resolution evidence from southern China of an early Holocene optimum and a mid-Holocene dry event during the past 18,000 years. *Quatern. Res.* **62**, 39–48 (2004).
33. Z. Ma, J. Huang, Y. Wei, J. Li, C. Hu, Organic carbon isotope records of the Poyang Lakes sediments and their implications for the paleoclimate during the last 8 ka. *Geochimica* **33**, 279–285 (2004).
34. W. Zhong, J. Cao, J. Xue, J. Ouyang, A 15,400-year record of climate variation from a subalpine lacustrine sedimentary sequence in the western Nanling Mountains in South China. *Quatern. Res.* **84**, 246–254 (2015).
35. Y. Cai, X. Cheng, L. Ma, R. Mao, S. F. M. Breitenbach, H. Zhang, G. Xue, H. Cheng, R. L. Edwards, Z. An, Holocene variability of East Asian summer monsoon as viewed from the speleothem $\delta^{18}O$ records in central China. *Earth Planet. Sci. Lett.* **558**, 116758 (2021).
36. T. Long, J. Qin, P. Atahan, S. Mooney, D. Taylor, Rising waters: New geoarchaeological evidence of inundation and early agriculture from former settlement sites on the southern Yangtze Delta, China. *Holocene* **24**, 546–558 (2014).
37. L. Deng, Y. Liu, J. He, R. Jiang, F. Jiang, J. Chen, Z. Chen, Q. Sun, New archaeobotanical evidence reveals synchronous rice domestication 7600 years ago on south Hangzhou Bay coast, eastern China. *Anthropocene* **33**, 100280 (2021).
38. D. Q. Fuller, L. Qin, Y. Zheng, Z. Zhao, X. Chen, L. A. Hosoya, G.-P. Sun, The domestication process and domestication rate in rice: Spikelet bases from the Lower Yangtze. *Science* **323**, 1607–1610 (2009).
39. G. Ling, C. Ma, Q. Yang, Z. Hu, H. Zheng, B. Liu, N. Wang, M. Chen, Y. Zhao, Landscape evolution in the Liangzhu area since the early Holocene: A comprehensive sedimentological approach. *Palaeogeogr. Palaeoclimatol. Palaeoecol.* **562**, 110141 (2021).
40. Y. Liu, Q. Sun, I. Thomas, L. Zhang, B. Finlayson, W. Zhang, J. Chen, Z. Chen, Middle Holocene coastal environment and the rise of the Liangzhu City complex on the Yangtze delta, China. *Quatern. Res.* **84**, 326–334 (2015).
41. Y. Liu, L. Deng, J. He, X. Zhao, H. Wang, D. Feng, J. Chen, M. Li, Q. Sun, Holocene geomorphological evolution and the Neolithic occupation in South Hangzhou Bay, China. *Geomorphology* **389**, 107827 (2021).
42. C. Zhu et al., Recognition of sea-level change during the Neolithic period in the Jiangsu Area, East China. *Chin. Sci. Bull.* **61**, 374–387 (2016).
43. L. Wu, S. Lu, C. Zhu, C. Ma, X. Sun, X. Li, C. Li, Q. Guo, Holocene environmental archaeology of the Yangtze river valley in China: A review. *Landarzt* **10**, 302 (2021).
44. Q. Sun, Y. Liu, B. Wünnemann, Y. Peng, X. Jiang, L. Deng, J. Chen, M. Li, Z. Chen, Climate as a factor for Neolithic cultural collapses approximately 4000 years BP in China. *Earth Sci. Rev.* **197**, 102915 (2019).
45. Group of The Xia-Shang-Zhou Chronology Project, *The Xia-Shang-Zhou Chronology Project Report for the Years 1996–2000 (Abridged)* (World Book Publishing Company, Beijing, 2000).
46. L. Tan, C.-C. Shen, Y. Cai, H. Cheng, R. L. Edwards, Great flood in the middle-lower Yellow River reaches at 4000 a BP inferred from accurately-dated stalagmite records. *Sci. Bull.* **63**, 206–208 (2018).

47. S. Xie, R. P. Evershed, X. Huang, Z. Zhu, R. D. Pancost, P. A. Meyers, L. Gong, C. Hu, J. Huang, S. Zhang, Y. Gu, J. Zhu, Concordant monsoon-driven postglacial hydrological changes in peat and stalagmite records and their impacts on prehistoric cultures in central China. *Geology* **41**, 827–830 (2013).

48. Z. Zhu, J. M. Feinberg, S. Xie, M. D. Bourne, C. Huang, C. Hu, H. Cheng, Holocene ENSO-related cyclic storms recorded by magnetic minerals in speleothems of central China. *Proc. Natl. Acad. Sci. U.S.A.* **114**, 852–857 (2017).

49. L. Tan, C. Hu, H. Cheng, L. R. Edwards, Y. Gao, H. Xu, H. Zhang, Z. An, Centennial-to-decadal-scale monsoon precipitation variations in the upper Hanjiang River region, China over the past 6650 years. *Earth Planet. Sci. Lett.* **482**, 580–590 (2018).

50. C. M. Moy, G. O. Seltzer, D. T. Rodbell, D. M. Anderson, Variability of El Niño/Southern Oscillation activity at millennial timescales during the Holocene epoch. *Nature* **420**, 162–165 (2002).

51. R. L. Edwards, J. Chen, G. Wasserburg, ^{238}U–^{234}U–^{230}Th–^{232}Th systematics and the precise measurement of time over the past 500,000 years. *Earth Planet. Sci. Lett.* **81**, 175–192 (1987).

52. H. Cheng, R. L. Edwards, J. Hoff, C. D. Gallup, D. A. Richards, Y. Asmerom, The half-lives of uranium-234 and thorium-230. *Chem. Geol.* **169**, 17–33 (2000).

53. H. Cheng, R. L. Edwards, C.-C. Shen, V. J. Polyak, Y. Asmerom, J. Woodhead, J. Hellstrom, Y. Wang, X. Kong, C. Spötl, X. Wang, E. Calvin Alexander Jr., Improvements in ^{230}Th dating, ^{230}Th and ^{234}U half-life values, and U–Th isotopic measurements by multi-collector inductively coupled plasma mass spectrometry. *Earth Planet. Sci. Lett.* **371-372**, 82–91 (2013).

54. S. F. M. Breitenbach, B. Goswami, J. U. L. Baldini, H. E. Ridley, D. J. Kennett, K. M. Prufer, V. V. Aquino, Y. Asmerom, V. J. Polyak, H. Cheng, J. Kurths, N. Marwan, Constructing proxy records from age models (COPRA). *Clim. Past.* **8**, 1765–1779 (2012).

55. C. Spötl, Long-term performance of the Gasbench isotope ratio mass spectrometry system for the stable isotope analysis of carbonate microsamples. *Rapid Commun. Mass Spectrom.* **25**, 1683–1685 (2011).

56. L. Stott, K. Cannariato, R. Thunell, G. H. Haug, A. Koutavas, S. Lund, Decline of surface temperature and salinity in the western tropical Pacific Ocean in the Holocene epoch. *Nature* **431**, 56–59 (2004).

57. G. H. Haug, K. A. Hughen, D. M. Sigman, L. C. Peterson, U. Röhl, Southward migration of the intertropical convergence zone through the Holocene. *Science* **293**, 1304–1308 (2001).

58. A. Berger, Long-term variations of caloric insolation resulting from the Earth's orbital elements. *Quatern. Res.* **9**, 139–167 (1978).

59. C. Hu, G. M. Henderson, J. Huang, S. Xie, Y. Sun, K. R. Johnson, Quantification of Holocene Asian monsoon rainfall from spatially separated cave records. *Earth Planet. Sci. Lett.* **266**, 221–232 (2008).

60. C.-J. Chen, D.-X. Yuan, J.-Y. Li, X.-F. Wang, H. Cheng, Y.-F. Ning, R. L. Edwards, Y. Wu, S.-Y. Xiao, Y.-Z. Xu, Y.-Y. Huang, H.-Y. Qiu, J. Zhang, M.-Q. Liang, T.-Y. Li, The 4.2 ka event in East Asian monsoon region, precisely reconstructed by multi-proxies of stalagmite, in *Climate of the Past Discussions* (2021), p. 1.

61. Y. Zhang, C. C. Huang, J. Pang, X. Zha, Y. Zhou, H. Gu, Holocene paleofloods related to climatic events in the upper reaches of the Hanjiang River valley, middle Yangtze River basin, China. *Geomorphology* **195**, 1–12 (2013).

62. L. Tan, Y. Li, X. Wang, Y. Cai, F. Lin, H. Cheng, L. Ma, A. Sinha, R. L. Edwards, Holocene monsoon change and abrupt events on the western Chinese Loess Plateau as revealed by accurately-dated stalagmites. *Geophys. Res. Lett.* **46**, e2020GL090273 (2020).

63. J. Dong, C.-C. Shen, X. Kong, H.-C. Wang, X. Jiang, Reconciliation of hydroclimate sequences from the Chinese Loess Plateau and low-latitude East Asian Summer Monsoon regions over the past 14,500 years. *Palaeogeogr. Palaeoclimatol. Palaeoecol.* **435**, 127–135 (2015).

64. Y. Li, Z. Rao, Q. Xu, S. Zhang, X. Liu, Z. Wang, H. Cheng, R. L. Edwards, F. Chen, Inter-relationship and environmental significance of stalagmite $\delta^{13}C$ and $\delta^{18}O$ records from Zhenzhu Cave, north China, over the last 130 ka. *Earth Planet. Sci. Lett.* **536**, 116149 (2020).

65. Y. Cai, L. Tan, H. Cheng, Z. An, R. L. Edwards, M. J. Kelly, X. Kong, X. Wang, The variation of summer monsoon precipitation in central China since the last deglaciation. *Earth Planet. Sci. Lett.* **291**, 21–31 (2010).

66. N. Zhang, Y. Yang, H. Cheng, J. Zhao, X. Yang, S. Liang, X. Nie, Y. Zhang, R. L. Edwards, Timing and duration of the East Asian summer monsoon maximum during the Holocene based on stalagmite data from North China. *Holocene* **28**, 1631–1641 (2018).

67. J. Dong, Y. Wang, H. Cheng, B. Hardt, R. L. Edwards, X. Kong, J. Wu, S. Chen, D. Liu, X. Jiang, K. Zhao, A high-resolution stalagmite record of the Holocene East Asian monsoon from Mt Shennongjia, central China. *Holocene* **20**, 257–264 (2010).

68. C. A. Dykoski, R. L. Edwards, H. Cheng, D. Yuan, Y. Cai, M. Zhang, Y. Lin, J. Qing, Z. An, J. Revenaugh, A high-resolution, absolute-dated Holocene and deglacial Asian monsoon record from Dongge Cave, China. *Earth Planet. Sci. Lett.* **233**, 71–86 (2005).

69. G. Bond, B. Kromer, J. Beer, R. Muscheler, M. N. Evans, W. Showers, S. Hoffmann, R. Lotti-Bond, I. Hajdas, G. Bonani, Persistent solar influence on North Atlantic climate during the Holocene. *Science* **294**, 2130–2136 (2001).

70. J. Xiao, S. Zhang, J. Fan, R. Wen, D. Zhai, Z. Tian, D. Jiang, The 4.2 ka BP event: Multi-proxy records from a closed lake in the northern margin of the East Asian summer monsoon. *Clim. Past* **14**, 1417–1425 (2018).

71. J. Xiao, B. Si, D. Zhai, S. Itoh, Z. Lomtatidze, Hydrology of Dali lake in central-eastern Inner Mongolia and Holocene East Asian monsoon variability. *J. Paleolimnol.* **40**, 519–528 (2008).

72. F. Chen, Q. Xu, J. Chen, H. J. B. Birks, J. Liu, S. Zhang, L. Jin, C. An, R. J. Telford, X. Cao, Z. Wang, X. Zhang, K. Selvaraj, H. Lu, Y. Li, Z. Zheng, H. Wang, A. Zhou, G. Dong, J. Zhang, X. Huang, J. Bloemendal, Z. Rao, East Asian summer monsoon precipitation variability since the last deglaciation. *Sci. Rep.* **5**, 11186 (2015).

73. J. Wu, Y. Wang, J. Dong, Changes in East Asian summer monsoon during the Holocene recorded by stalagmite $\delta^{18}O$ records from Liaoning Province. *Quat. Sci.* **31**, 990–998 (2011).

74. J. Zhao, L. Tan, Y. Yang, C. Pérez-Mejías, Y. A. Brahim, J. Lan, J. Wang, H. Li, T. Wang, H. Zhang, H. Cheng, New insights towards an integrated understanding of NE Asian monsoon during mid to late Holocene. *Quat. Sci. Rev.* **254**, 106793 (2021).

75. X. Yang, R. Liu, R. Zhang, B. Wang, R. Zhang, Y. Yan, A stalagmite $\delta^{18}O$ record from Jinfo Cave, southern China reveals early-mid holocene variations in the East Asian Summer Monsoon. *Quat. Int.* **537**, 61–68 (2020).

76. M. Zhang, D. Yuan, Y. Lin, J. Qin, L. Bin, H. Cheng, R. L. Edwards, A 6000-year high-resolution climatic record from a stalagmite in Xiangshui Cave, Guilin, China. *Holocene* **14**, 697–702 (2004).

77. C. Ma, C. Zhu, C. Zheng, C. Wu, Y. Guan, Z. Zhao, L. Huang, R. Huang, High-resolution geochemistry records of climate changes since late-glacial from Dajiuhu peat in Shennongjia Mountains, Central China. *Chin. Sci. Bull.* **53**, 28–41 (2008).

78. C. Huang, J. Pang, X. Zha, Y. Zhou, H. Su, Y. Li, Extraordinary floods of 4100–4000 a BP recorded at the Late Neolithic ruins in the Jinghe River gorges, Middle Reach of the Yellow River, China. *Palaeogeogr. Palaeoclimatol. Palaeoecol.* **289**, 1–9 (2010).

79. C. C. Huang, J. L. Pang, X. Zha, H. Su, Y. Jia, Extraordinary floods related to the climatic event at 4200 a BP on the Qishuihe River, middle reaches of the Yellow River, China. *Quat. Sci. Rev.* **30**, 460–468 (2011).

80. L. Wu, C. Zhu, C. Ma, F. Li, H. Meng, H. Liu, L. Li, X. Wang, W. Sun, Y. Song, Mid-Holocene palaeoflood events recorded at the Zhongqiao Neolithic cultural site in the Jianghan Plain, middle Yangtze River Valley, China. *Quat. Sci. Rev.* **173**, 145–160 (2017).